THE JOURNAL OF PHYSICAL CHEMISTRY B

Article

pubs.acs.org/JPCB

How Many Bubbles in Your Glass of Bubbly?

Gérard Liger-Belair*

Equipe Effervescence, Champagne et Applications, Groupe de Spectrométrie Moléculaire et Atmosphérique (GSMA), UMR CNRS 7331, UFR Sciences Exactes et Naturelles, Université de Reims Champagne-Ardenne, BP 1039, 51687 Reims Cedex 2, France

ABSTRACT: The issue about how many carbon dioxide bubbles are likely to nucleate in a glass of champagne (or bubbly) is of concern for sommeliers, wine journalists, experienced tasters, and any open minded physical chemist wondering about complex phenomena at play in a glass of bubbly. The whole number of bubbles likely to form in a single glass is the result of the fine interplay between dissolved CO_2, tiny gas pockets trapped within particles acting as bubble nucleation sites, and ascending bubble dynamics. Based on theoretical models combining ascending bubble dynamics and mass transfer equations, the falsely naïve question of how many bubbles are likely to form per glass is discussed in the present work. A theoretical relationship is derived, which provides the whole number of bubbles likely to form per glass, depending on various parameters of both the wine and the glass itself.

1. INTRODUCTION

Since the end of the 17th century, champagne has been a worldwide renowned French sparkling wine. Nevertheless, only since the past decade has much research been devoted to depict each and every parameter involved in its bubbling process (the highly sought-after and so-called *effervescence* process).[1] In champagne and sparkling wine tasting, effervescence is indeed a crucial parameter since it directly impacts the three following sensory properties: (i) the visual perception of the wine itself, always preceding the action of inhaling and tasting it,[2] (ii) the aromatic perception of the wine as bursting bubbles release gaseous carbon dioxide (CO_2) and volatile organic compounds above the wine surface,[3−5] and (iii) the mouth feel sensation, as dissolved CO_2 and collapsing bubbles in the oral cavity act on both trigeminal receptors,[6−8] and gustatory receptors.[9,10]

From a strictly chemical point of view, champagne wines are multicomponent hydroalcoholic systems, with a density close to unity, a surface tension $\gamma \approx 50$ mN m^{-1} (indeed highly ethanol-dependent), and a viscosity about 50% larger than that of pure water (also mainly due to the presence of 12.5% (v/v) ethanol).[2] Champagne wines are supersaturated with dissolved CO_2, formed together with ethanol during a second fermentation process, called *prise de mousse* (promoted by adding yeasts and sugar inside bottles filled with a base wine and sealed with a cap). Champagnes, or sparkling wines elaborated through the same traditional method, therefore hold a concentration of dissolved CO_2 proportional to the level of sugar added to promote this second fermentation. The process of fermentation was first scientifically described by the French chemist Joseph-Louis Gay Lussac in 1810, when he demonstrated that glucose is the basic starting block for producing ethanol and gaseous CO_2:

$$C_6H_{12}O_6 \rightarrow 2CH_3CH_2OH + 2CO_2 \quad (1)$$

Traditionally, 24 g/L of sugar are added in the base wine to promote the *prise de mousse*. Following eq 1, 24 g/L of sugar added in closed bottles to promote the second alcoholic fermentation produce approximately 11.8 g of CO_2/(L of wine). The concentration of dissolved CO_2 in champagne (in grams per liter) is therefore roughly equivalent to half of the concentration of sugar (in grams per liter) added into the base wine in order to promote the *prise de mousse*.[11] Experiments with early disgorged champagne samples were done recently. The characteristic concentration of dissolved CO_2 measured inside freshly opened standard bottles was found to be of the order of 11.5 g L^{-1}, and therefore in very good accordance with what is expected from fermenting 24 g L^{-1} of sugar to promote the *prise de mousse* in the sealed bottles.[12−14]

As soon as a bottle of champagne or sparkling wine is uncorked, the liquid phase becomes supersaturated with dissolved CO_2 (since ambient air contains only traces of gaseous CO_2). To reach a new stable thermodynamic state with regard to CO_2, champagne must therefore progressively degas. It is worth noting that desorbing about 11.5 g L^{-1} of dissolved CO_2 corresponds to the release of approximately 5 L of gaseous CO_2/(standard 75 cL bottle), at standard temperature and pressure. Generally speaking, a link has been recently evidenced between carbonation and the release of some aroma compounds in carbonated waters.[15,16] Sensory analysis results indeed revealed for example that the presence of CO_2 increased aroma perception in mint-flavored carbonated beverages.[16] Even more recently, experiments conducted under standard tasting conditions revealed that the concentration of gaseous ethanol above champagne glasses was highly enhanced if the glass shows effervescence, thus pointing out the crucial role of

Received: January 10, 2014
Revised: February 17, 2014
Published: February 26, 2014

bursting bubbles in champagne tasting.[17] In fact, as champagne is poured into a glass, the myriad of ascending and bursting bubbles radiate a multitude of tiny droplets above the free surface, into the form of very characteristic aerosols, as shown in the photograph displayed in Figure 1. Quite recently,

Figure 1. Hundreds of bubbles simultaneously bursting at the surface of a glass poured with bubbly, thus projecting hundreds of tiny droplets above the liquid surface into the form of a very characteristic aerosol. Photograph by Alain Cornu/Collection CIVC.

ultrahigh-resolution mass spectrometry was used in order to analyze the aerosols released by champagne bubbles.[18] In comparison with the champagne bulk, champagne droplets were found to be overconcentrated with various surface active compounds, some of them showing indeed aromatic properties. This very characteristic fizz is therefore strongly believed to enhance the flavor sensation above a glass of bubbly in comparison with that above a glass of flat wine. Moreover, glass shape was also found to play a role concerning the kinetics of dissolved CO_2 and ethanol release under standard tasting conditions.[19] Nevertheless, it is worth noting that a high level of inhaled gaseous CO_2 may also become an irritant in the nasal cavity.[20,21] For all of the aforementioned reasons, suffice it to say that the interplay between dissolved CO_2 and ascending CO_2 bubbles in champagne, sparkling wines, and carbonated beverages in general, coupled with several tasting conditions, leads to modifications of the neuro-physicochemical mechanisms responsible for mouth feel, aroma release, and flavor perception.

Following these recent highlights, the issue about the whole number of CO_2 bubbles formed per glass is of concern for sommeliers, wine journalists, experienced tasters, and any open minded person wondering about complex phenomena at play in a glass of champagne (or bubbly). To get an idea of how many bubbles are potentially involved all along the degassing process from a single glass, a rough approach would consist of simply dividing the 5 L of gaseous CO_2 dissolved into a single 75 cL bottle by the average volume of a typical bubble of 0.5 mm in diameter. A huge number close to 100 million is found! Since it is usually admitted that seven flutes can be served from a single 75 cl champagne bottle, approximately 15 million bubbles should be able to form in a glass. This rough order of magnitude is the answer often given in wine blogs and magazines to our preceding issue concerning the whole number of bubbles likely to form into a single glass of bubbly. Nevertheless, this rough estimation is indeed far from correct for two main reasons. First, all of the dissolved CO_2 which escapes from your glass bubbly does not form bubbles, and second, the size of bubbles continuously decreases as time proceeds. Based on theoretical models combining ascending bubble dynamics and mass transfer equations, the question of how many bubbles are likely to form into a single glass of bubbly is discussed step by step in the present work.

2. REQUIRED BACKGROUND

2.1. Temperature Dependence of CO_2 Solubility in Champagne. Generally speaking, the solubility of gas species in a liquid phase is strongly temperature-dependent (the lower the temperature of the solution, the higher the gas solubility). Thermodynamically speaking, the solubility of gaseous CO_2 in wine was found to be conveniently expressed with a van't Hoff like equation as follows:[2]

$$k_H(T) = k_{298K} \exp\left[-\frac{\Delta H_{diss}}{R}\left(\frac{1}{T} - \frac{1}{298}\right)\right] \quad (2)$$

with k_{298K} being the Henry's law constant of dissolved CO_2 in champagne (its solubility) at 298 K ($\approx 2.75 \times 10^{-4}$ mol m^{-3} Pa^{-1} $\approx$ 1.21 g L^{-1} bar^{-1}), ΔH_{diss} being the dissolution enthalpy of CO_2 in the liquid phase (J mol^{-1}), R being the ideal gas constant (8.31 J K^{-1} mol^{-1}), and T being the absolute temperature (K). The best fit to experimental data was found with $\Delta H_{diss} \approx -24800$ J mol^{-1}.[2]

2.2. Critical Radius Required for Bubble Nucleation. Thermodynamically speaking, bubble formation in a liquid phase is limited by an energy barrier to overcome (for an exhaustive review see the study by Lugli and Zerbetto,[22] and references therein). Jones et al.[23] made a classification of the broad range of the various nucleation types likely to be encountered in liquids supersaturated with dissolved gas. Following their nomenclature, classical homogeneous bubble nucleation within the liquid bulk,[24,25] and heterogeneous bubble nucleation on perfectly smooth surfaces (i.e, nucleation without the help of any preexisting gas cavity[26,27]) are referred to as type I and II nucleation, respectively. Pseudoclassical heterogeneous bubble nucleation—referred to as bubble nucleation from a preexisting gas pocket with a radius of curvature smaller than a critical radius classically defined as $r^* = -2\gamma/G_v$ (with γ being the liquid/gas surface tension and G_v being the Gibbs free energy per unit volume for phase change)—is called type III bubble nucleation. Finally, following their nomenclature, nonclassical heterogeneous bubble nucleation from preexisting gas cavities with radii larger than the critical radius is referred to as type IV bubble nucleation.

In weakly supersaturated liquids such as champagne, sparkling wines, and carbonated beverages in general, bubbles do not just pop into existence *ex nihilo*. Type I and II bubble nucleation are therefore thermodynamically forbidden, since they both require much higher levels of dissolved CO_2 than those classically found in carbonated beverages. Even type III bubble nucleation is very unlikely to occur, unless preexisting gas cavities show radii very close to the critical radius. This is

dx.doi.org/10.1021/jp500295e | J. Phys. Chem. B 2014, 118, 3156−3163

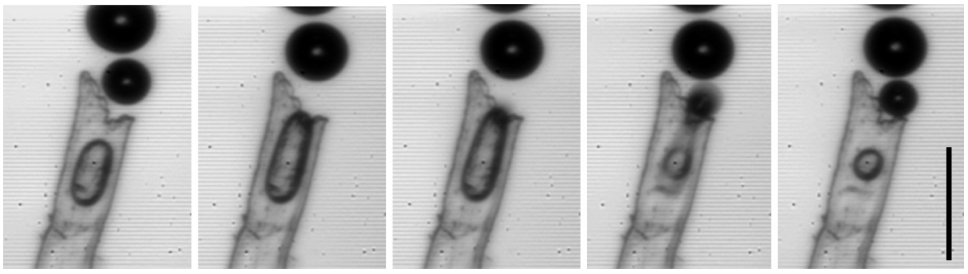

Figure 2. Time sequence showing the nucleation of a bubble from the tip of a very typical cellulose fiber stuck on the wall of a glass poured with champagne (bar = 100 μm).

the reason why, in weakly supersaturated liquids such as bubblies, bubble formation and growing require preexisting gas cavities with radii of curvature large enough to overcome the nucleation energy barrier and grow freely (i.e., type IV bubble nucleation).[28] This critical radius, denoted r^*, can easily be accessed by using standard thermodynamic arguments or by using simple arguments based on classical diffusion principles.[29] The r^* required to enable type IV bubble nucleation in champagne and sparkling wines expresses as follows:

$$r^* \approx \frac{2\gamma k_H}{(c_L - k_H P_0)} \tag{3}$$

with γ being the surface tension of the wine (typically of the order of 50 mN m^{-1} in champagne and sparkling wines), P_0 being the atmospheric pressure ($\approx 10^5$ N m$^{-2} \approx 1$ bar), and c_L being the concentration of dissolved CO_2 found in the liquid bulk (expressed in mol m^{-3}).

Following eq 3 with k_H given in eq 2, and assuming a concentration of dissolved CO_2 within the champagne bulk of 11.5 g L^{-1} (i.e., $c_L \approx 260$ mol m^{-3}), the critical radius required to enable type IV bubble nucleation is therefore of the order of 0.2 μm at a drinking temperature of 10 °C.

2.3. Bubble Nucleation from Gas Cavities in Champagne Glasses. Closer inspection of glasses poured with champagne, sparkling wines, or any other sparkling beverage, such as beer for example, was conducted through a high-speed video camera fitted with a microscope objective.[29−33] It revealed that most of the bubble nucleation sites were found to be located on preexisting gas cavities trapped within hollow and roughly cylindrical cellulose-fiber-made structures on the order of 100 μm long with a cavity mouth of several micrometers. The hollow cavity (a kind of tiny channel within the fibers) where a gas pocket is trapped during the pouring process is called the *lumen*.[31] It can be clearly noticed from Figure 2 that the radius of curvature of the gas pocket trapped within the fiber's lumen is much higher than the aforementioned critical radius r^* required for type IV bubble nucleation. In previous works, by retrieving mass transfer equations in diffusion−convection conditions, the frequency of bubble nucleation from such a cylindrical gas pocket growing trapped inside a fiber's lumen was modeled and found to be in good agreement with experimental data.[31−35]

2.4. Ascending Bubble Dynamics. A very typical high-speed photograph of a single bubble train showing bubbles released with clockwork regularity from a single nucleation site is displayed in Figure 3. Bubbles are seen growing in size while ascending through the liquid phase supersaturated with dissolved CO_2, as first reported in a glass of beer by Shafer and Zare.[36] By using ascending bubble dynamics coupled with mass transfer equations, the following relationship was derived,

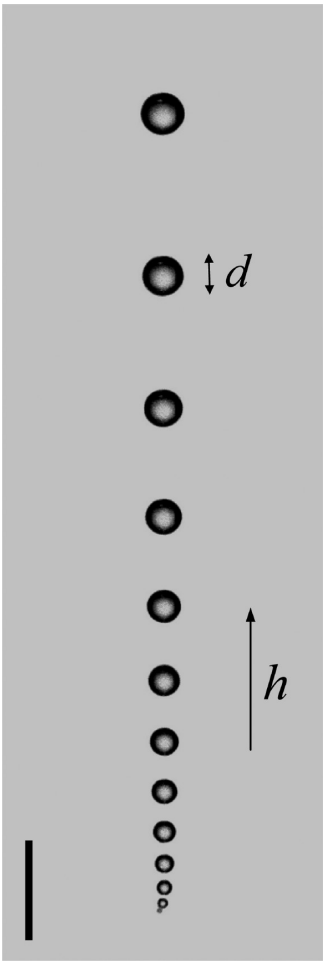

Figure 3. High-speed photograph showing bubbles rising in line and growing in size while ascending toward the champagne surface (bar = 1 mm).

which links the diameter d of a CO_2 bubble rising in a liquid phase supersaturated with dissolved CO_2, with some physicochemical parameters of the liquid phase (in the MKS system of units),[2]

$$d \approx 5.4 \times 10^{-3} T^{5/9} \left(\frac{1}{\rho g}\right)^{2/9} \left(\frac{c_L - k_H P_0}{P_0}\right)^{1/3} h^{1/3} \tag{4}$$

with ρ being the champagne density ($\approx 10^3$ kg m^{-3}), g being the acceleration due to gravity (≈ 9.8 m s^{-2}), and h being the distance traveled by a bubble from its nucleation site to the champagne free surface.

dx.doi.org/10.1021/jp500295e | J. Phys. Chem. B 2014, 118, 3156−3163

Figure 4. Photographs of vertical and tilted flute pouring. Champagne can be poured straight down the middle of a vertically oriented flute (a) or down the side of a tilted flute (b), with significant differences in the concentration of dissolved CO_2 found within the champagne after serving it.

It is worth noting that, to propose the previous relationship which provides the diameter of a champagne bubble with several parameters of the liquid phase, ascending bubbles were considered as rigid spheres (i.e., hydrodynamically speaking, the boundary conditions on the bubble surface are reduced from slip to nonslip due to surface active compounds forbidding interfacial mobility). Moreover, in eq 4, the concentration c_L of dissolved CO_2 is implicitly considered as being constant all along the vertical distance traveled by the rising bubble. This assumption is nevertheless reasonable, because ascending bubble-driven flow patterns quickly develop in the whole liquid bulk, as revealed in previous works through laser tomography techniques.[37,38] Continuous, and vigorous recirculation of the liquid phase in champagne glasses therefore most probably forbids the formation of zones depleted with dissolved CO_2 around ascending bubble trains.

Following eq 4, the volume of a CO_2 bubble which reaches the liquid surface before bursting therefore finally expresses as follows:

$$v_b \approx \frac{d^3}{2} \approx 7.9 \times 10^{-8} T^{5/3} \left(\frac{1}{\rho g}\right)^{2/3} \left(\frac{c_L - k_H P_0}{P_0}\right) h \qquad (5)$$

Since, as shown in the latter expression, the volume of a bubble is strongly dependent on several parameters, including the champagne temperature, the total number of bubbles likely to form in a single glass is therefore also expected to depend on those parameters. The aim of the following paragraph is to discuss the dependence on these parameters of the whole number of bubbles likely to form per glass.

3. DISCUSSION

3.1. Initial Concentration of Dissolved CO_2 Found in the Glass. As already shown in recent papers, pouring champagne into a glass is far from inconsequential with regard to dissolved CO_2 concentrations found in champagne.[39,40] During the several seconds of the pouring process, champagne undergoes highly turbulent flows with often numerous air bubble entrapments, even if it is served gently. Consequently, during the pouring step, champagne loses a very significant part of its initial content in dissolved CO_2. As a result, initial concentrations of dissolved CO_2 found in glasses after pouring are well below the typical dissolved CO_2 content of 11.5 g L^{-1} still found in the sealed bottles. Initial bulk concentrations of dissolved CO_2 after pouring, denoted c_I, were chemically accessed by using carbonic anhydrase,[41] for three various champagne temperatures, and depending on whether champagne was served in a vertical or in a tilted flute (as seen in Figure 4). As expected, champagne just dispensed in glasses was found to initially hold, after pouring, a concentration of dissolved CO_2 much lower than that in the sealed bottles.[39,40] Moreover, the concentration of dissolved CO_2 found within glasses was found to depend on both the champagne temperature and the way of serving it, as seen in the synthetic graph displayed in Figure 5. The temperature-dependent dissolved CO_2 data found within glasses after pouring were fitted with polynomial functions (for both ways of serving champagne). Very clearly, low temperatures, and tilting a glass while serving champagne, help preserve dissolved CO_2 within the wine.

3.2. Critical Concentration of Dissolved CO_2 as Bubbling Stops. As already shown experimentally, the frequency of bubble formation from a given nucleation site is found to progressively decrease with time, because the concentration of dissolved CO_2 progressively decreases as CO_2 continuously escapes from the liquid phase.[34] Furthermore, it is worth noting that the bubbling frequency of a given nucleation site vanishes (i.e., the bubble release ceases), as c_L reaches a finite value.[34] Actually, following both Laplace's and Henry's laws, the radius of curvature r of the gaseous CO_2 bubble trapped within the fiber's lumen forces in its close vicinity a concentration of dissolved CO_2 on the order of $c_B \approx k_H(P_0 + 2\gamma/r)$, as shown in Figure 6. It is worth noting that the contribution of hydrostatic pressure is simply negligible in the case of a standard glass filled with about 10 cm of champagne ($\rho g h \approx 10^3 \times 10 \times 10^{-1} \approx 10^3$ Pa $\ll P_0$). Consequently, as the dissolved CO_2 concentration found in the champagne bulk, i.e., c_L, reaches the dissolved CO_2 concentration found in the close vicinity of the gas pocket trapped within the fiber, i.e., c_B, bubble nucleation stops simply because the driving force of molecular diffusion vanishes. Therefore, as the concentration of dissolved CO_2 found in the liquid bulk reaches the critical value

dx.doi.org/10.1021/jp500295e | J. Phys. Chem. B 2014, 118, 3156−3163

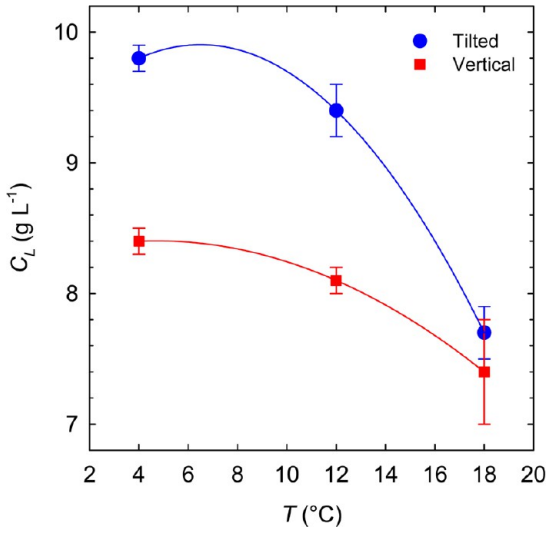

Figure 5. Concentrations of dissolved CO_2 found within 100 mL of champagne just dispensed in a classical flute (as that displayed in Figure 4) depending on whether champagne was served in a vertical or in a tilted flute. The level of champagne dispensed reaches 7.4 cm height in the flute; three various champagne temperatures were investigated (namely, 4, 12, and 18 °C) (redrawn from ref 39); temperature-dependent experimental data were fitted with polynomial functions, which appear as red and blue dashed lines, respectively.

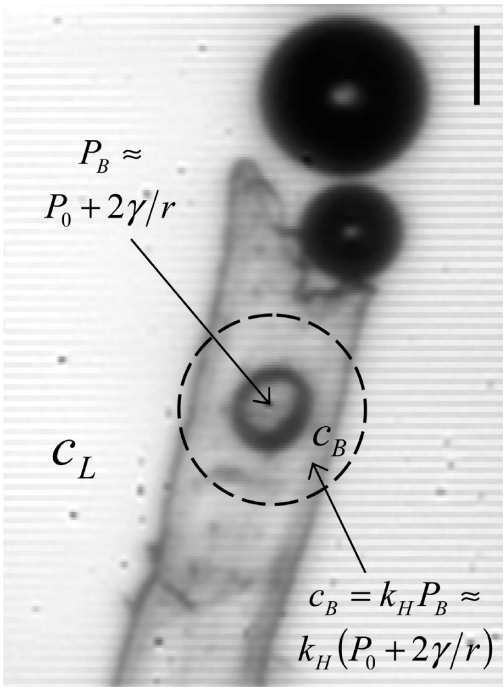

Figure 6. Close-up view of a tiny cellulose fiber acting as a bubble nucleation site in a glass of champagne. The capillary pressure existing in the gaseous CO_2 pocket trapped within the fiber's lumen forces a finite and temperature-dependent concentration of dissolved CO_2 in a boundary layer surrounding the gas pocket (bar = 20 μm).

c_L^* expressed hereafter, diffusion of dissolved CO_2 toward the gas pocket ceases and the nucleation site stops releasing bubbles:

$$c_L^* = c_B \approx k_H\left(P_0 + \frac{2\gamma}{r}\right) \quad (6)$$

It is worth noting that c_L^* is highly temperature-dependent, simply because the dissolved CO_2 solubility k_H is indeed highly temperature-dependent, as seen in eq 2. For example, the critical concentration c_L^*, below which bubble release becomes thermodynamically impossible from the fiber displayed in Figure 2, is therefore $c_L^* \approx k_H(P_0 + 2\gamma/r) \approx 2.07 \times 10^{-5}(10^5 + 2 \times 5 \times 10^{-2}/10^{-5}) \approx 2.3$ g L^{-1}, at 4 °C, whereas it is only $c_L^* \approx 1.54 \times 10^{-5}(10^5 + 2 \times 5 \times 10^{-2}/10^{-5}) \approx 1.7$ g L^{-1}, at 18 °C.

3.3. Theoretical Determination of the Whole Number of Bubbles Likely To Form in a Single Glass. The assumption is made that a flute is poured with a level h of champagne, and with an arbitrary number of identical nucleation sites lying on the bottom of the flute, as shown in the photograph displayed in Figure 7. Strictly speaking, there

Figure 7. Photograph of a typical flute showing bubbles nucleating on the bottom of the flute and rising toward the champagne surface. Photograph by Alain Cornu/Collection CIVC.

are two mechanisms for gaseous CO_2 losses under standard tasting conditions: (i) losses due to diffusion through the surface of the liquid (invisible to the naked eye) and (ii) losses due to bubbling (the very much sought-after and so-called effervescence process).[42] Per unit of time, the volume of gaseous CO_2 exclusively lost due to bubbling is simply accessed by multiplying the frequency of bubble formation in the glass (equivalent indeed to the frequency of bubbles bursting at the champagne surface, under steady state conditions) by the volume, v_b, of a bubble which reaches the champagne surface, as defined in eq 5. But, in fact, experimental data proved that in a classic crystal flute, contrary to what could have been expected, only about 20% of carbon dioxide escapes in the form of bubbles, whereas the other 80% escapes directly through the free surface of champagne.[42] Actually, because only about 20% of dissolved CO_2 escapes in the form of bubbles, the total volume of gaseous CO_2 escaping from the flute, per unit of time, may be expressed in a differential form as follows:

dx.doi.org/10.1021/jp500295e | J. Phys. Chem. B 2014, 118, 3156−3163

$$\frac{dv}{dt} \approx 5v_b \frac{dN}{dt} \quad (7)$$

Therefore, per unit of time, it is worth noting that champagne loses a concentration of dissolved CO_2 (expressed in mol m^{-3}), both through bursting bubbles and through invisible diffusion through the free surface, which may be expressed as follows,

$$\frac{dc}{dt} = \frac{1}{V_M V_L}\frac{dv}{dt} \approx \frac{5v_b}{V_M V_L}\frac{dN}{dt} \quad (8)$$

with V_L being the volume of champagne served into the glass (given in m^3), and V_M being the molar volume of an ideal gas (i.e., RT/P_0, given in m^3).

Time can be eliminated from eq 8, and the whole number N of bubbles likely to form in the glass during the whole degassing process is expressed as

$$N = \int_{c_L^*}^{c_I} \frac{V_M V_L}{5v_b}\, dc = \frac{RTV_L}{5P_0}\int_{c_L^*}^{c_I} \frac{dc}{v_b} \quad (9)$$

with c_I being the initial concentration of dissolved CO_2 found in champagne immediately after the pouring step and c_L^* being the critical concentration of dissolved CO_2 found in champagne as the bubbling stops from the bubble nucleation sites lying on the bottom of the glass.

By replacing v_b in the previous equation by its theoretical relationship given in eq 5, the whole number of bubbles likely to form in the glass my be rewritten as

$$N \approx \frac{2.6 \times 10^6 R V_L}{h}\left(\frac{\rho g}{T}\right)^{2/3}\int_{c_L^*}^{c_I} \frac{dc}{(c_L - k_H P_0)} \quad (10)$$

It is worth noting that the number of bubbles defined in eq 10 is a lower limit for the total number of bubbles likely to form in a single flute. Actually, bubble nucleation sites were all supposed to lie on the glass bottom (i.e., under a depth level h of champagne), thus producing the biggest possible bubble volume as they reach the champagne surface after a maximal distance traveled through the liquid phase supersaturated with dissolved CO_2.

Integrating the previous relationship, and replacing R by its numerical value, provides the following relationship:

$$N \approx \frac{2 \times 10^7 V_L}{h}\left(\frac{\rho g}{T}\right)^{2/3} \ln\left(\frac{c_I - k_H P_0}{c_L^* - k_H P_0}\right) \quad (11)$$

Replacing c_L^* by its expression given in eq 6 and replacing ρ and g by their respective numerical value finally lead to the following relationship, which provides the total number of bubbles likely to form in the glass, as a function of various parameters depending on both glass and wine properties:

$$N \approx \frac{10^{10} V_L}{h(273 + T)^{2/3}} \ln\left(\frac{r(c_I - k_H P_0)}{2k_H \gamma}\right) \quad (12)$$

with V_L being expressed in m^3, T in °C, h in m, r in m, c_I in mol m^{-3}, P_0 in Pa, k_H in mol m^{-3} Pa^{-1}, and γ in N m^{-1}.

c_I and k_H being highly temperature-dependent, N is therefore expected to depend on the tasting temperature of champagne. Finally, replacing in eq 12 each and every parameter by its numerical value, c_I by its temperature-dependent polynomial function drawn in Figure 5, and k_H by its van't Hoff like eq 2, the temperature-dependent number of bubbles likely to nucleate in your flute can be determined, whether the 100 mL of champagne are served in a vertical or in a tilted flute (see Figure 8). One million bubbles seems to be a reasonable approximation for the whole number of bubbles likely to form if you resist drinking champagne from your flute. As seen in Figure 8, depending on the champagne temperature, several tens of thousands bubbles may nevertheless be "saved" if champagne is served in a tilted flute.

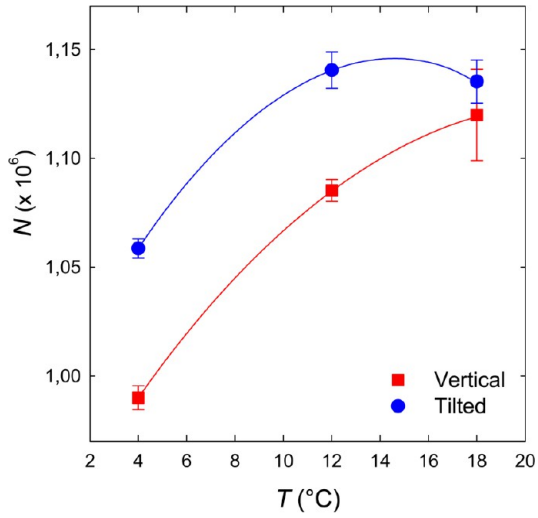

Figure 8. Temperature dependence of the theoretical number N of bubbles likely to nucleate in a single flute poured with 100 mL of champagne, whether champagne is served in a vertical or in a tilted flute.

Moreover, and interestingly, the global number of bubbles likely to nucleate in a flute increases with the champagne temperature. This result could first appear rather counter-intuitive for two reasons. First, the volume of a single bubble increases with the champagne temperature, and second, the initial concentration of dissolved CO_2 found in the flute after pouring decreases with the champagne temperature. Therefore, as the champagne temperature increases, the whole volume of CO_2 found within the flute decreases and is released into the form of bubbles whose volume increases with the champagne temperature. Naively, the whole number of bubbles likely to form in a flute was thus expected to decrease as the champagne temperature increases. Nevertheless, as seen in section 3.2, the critical concentration c_L^* below which bubble nucleation becomes thermodynamically impossible decreases with increasing champagne temperature. Actually, decreasing this critical concentration increases indeed the number of tiny bubbles likely to form, because the bubble volume decreases with the concentration of dissolved CO_2, as shown in eq 5. Now, while increasing the temperature of champagne, it happens that the number of tiny bubbles likely to form in a range of low dissolved CO_2 concentrations overcomes the number of bigger bubbles likely to form in the same range of high dissolved CO_2 concentrations found with low champagne temperatures early after pouring.

4. CONCLUSION

In conclusion, based on recently derived models which combine ascending bubble dynamics with mass transfer equations, the falsely naïve question of how many bubbles are likely to form into a single glass of champagne (or bubbly) was discussed. A theoretical relationship was derived which

dx.doi.org/10.1021/jp500295e | J. Phys. Chem. B 2014, 118, 3156−3163

provides the whole number of bubbles likely to form per glass, depending on various parameters of both the wine and the glass itself. If 100 mL of champagne are poured straight down the middle of a vertically oriented flute, about one million bubbles are likely to nucleate if you resist drinking from your flute. Otherwise, if champagne is more gently served on the wall of a tilted flute, dissolved CO_2 is better preserved, and therefore several tens of thousands of bubbles should additionally form. Interestingly, the theoretical number of bubbles likely to form was found to globally increase with the champagne temperature.

AUTHOR INFORMATION

Corresponding Author

*Tel.: 00 (33) 3 26 91 32 58. Fax: 00 (33) 3 26 91 31 47. E-mail: gerard.liger-belair@univ-reims.fr.

Notes

The authors declare no competing financial interest.

ACKNOWLEDGMENTS

Thanks are due to the Europôl'Agro institute and to the Association Recherche Oenologie Champagne Université for financial support. G.L.-B. warmly thanks Coopérative Nogent l'Abbesse, as well as Champagne Houses Pommery, and Veuve Clicquot Ponsardin, for regularly supplying us with various champagne samples. G.L.-B. is also indebted to the CNRS, the Région Champagne-Ardenne, the Ville de Reims, and the Conseil Général de la Marne for supporting our team and research.

NOMENCLATURE

c_B concentration of dissolved CO_2 in the close vicinity of the gas pocket trapped within the fiber's lumen (see Figure 6), mol m^{-3}

c_I initial concentration of dissolved CO_2 found in the liquid bulk after pouring champagne in the glass, mol m^{-3}

c_L concentration of dissolved CO_2 found in the liquid bulk, mol m^{-3}

c_L^* critical concentration of dissolved CO_2 found in the liquid bulk as bubbling stops, mol m^{-3}

d ascending bubble diameter, m

g acceleration due to gravity, $\approx$9.8 m s^{-2}

G_v Gibbs free energy per unit volume for phase change, J m^{-3}

h distance traveled by a bubble from its nucleation site to the champagne free surface, m

k_H Henry's law constant of dissolved CO_2 in champagne (its solubility), mol m^{-3} Pa^{-1}

k_{298K} Henry's law constant of dissolved CO_2 in champagne at 298 K, $\approx 2.75 \times 10^{-4}$ mol m^{-3} Pa^{-1}

N number of bubbles likely to nucleate per glass

P_0 atmospheric pressure, $\approx 10^5$ N m^{-2} = 1 bar

r^* critical radius required to enable bubble production, m

r radius of curvature of the gaseous CO_2 bubble trapped within the fiber's lumen, m

R ideal gas constant, = 8.31 J K^{-1} mol^{-1}

t time, s

T absolute temperature, K

v volume of gas phase CO_2, m^3

v_b bubble volume as it reaches the champagne surface, m^3

V_L volume of champagne served into the glass, m^3

V_M molar volume of an ideal gas (i.e., RT/P_0), m^3 mol^{-1}

γ liquid/gas surface tension, N m^{-1}

ΔH_{diss} dissolution enthalpy of gas phase CO_2 in the liquid phase, J mol^{-1}

ρ champagne density, $\approx 10^3$ kg m^{-3}

REFERENCES

(1) Liger-Belair, G. The science of bubbly. *Sci. Am.* **2003**, *288*, 80−85.

(2) Liger-Belair, G. The physics and chemistry behind the bubbling properties of champagne and sparkling wines: A state-of-the-art review. *J. Agric. Food Chem.* **2005**, *53*, 2788−2802.

(3) Priser, C.; Etievant, P. X.; Nicklaus, S.; Brun, O. Representative Champagne wine extracts for gas chromatography olfactometry analysis. *J. Agric. Food Chem.* **1997**, *45*, 3511−3514.

(4) Tominaga, T.; Guimbertau, G.; Dubourdieu, D. Role of certain volatile thiols in the bouquet of aged Champagne wines. *J. Agric. Food Chem.* **2003**, *51*, 1016−1020.

(5) Liger-Belair, G.; Conreux, A.; Villaume, S.; Cilindre, C. Monitoring the losses of dissolved carbon dioxide from laser-etched champagne glasses. *Food Res. Int.* **2013**, *54*, 516−522.

(6) Dessirier, J. M.; Simons, C.; Carstens, M.; O'Mahony, M.; Carstens, E. Psychophysical and neurobiological evidence that the oral sensation elicited by carbonated water is of chemogenic origin. *Chem. Senses* **2000**, *25*, 277−284.

(7) Kleeman, A.; Albrecht, J.; Schöpf, V.; Haegler, K.; Kopietz, R.; Hempel, J. M.; Linn, J.; Flanagin, V. L.; Fesl, G.; Wiesmann, M. Trigeminal perception is necessary to localize odors. *Physiol. Behav.* **2009**, *97*, 401−405.

(8) Meusel, T.; Negoias, S.; Scheibe, M.; Hummel, T. Topographical differences in distribution and responsiveness of trigeminal sensitivity within the human nasal mucosa. *Pain* **2010**, *151*, 516−521.

(9) Chandrashekar, J.; Yarmolinsky, D.; von Buchholtz, L.; Oka, Y.; Sly, W.; Ryba, N. J.; Zucker, C. S. The taste of carbonation. *Science* **2009**, *326*, 443−445.

(10) Dunkel, A.; Hofmann, T. Carbonic anhydrase IV mediates the fizz of carbonated beverages. *Angew. Chem., Int. Ed.* **2010**, *49*, 2975−2977.

(11) Liger-Belair, G.; Polidori, G.; Zéninari, V. Unraveling the evolving nature of gaseous and dissolved carbon dioxide in champagne wines: A state-of-the-art review, from the bottle to the tasting glass. *Anal. Chim. Acta* **2012**, *732*, 1−15.

(12) Autret, G.; Liger-Belair, G.; Nuzillard, J.-M.; Parmentier, M.; Dubois de Montreynaud, A.; Jeandet, P.; Doan, B. T.; Beloeil, J. C. Use of magnetic resonance spectrometry for the investigation of the CO_2 dissolved in champagne and sparkling wines: A non-destructive and non-intrusive method. *Anal. Chim. Acta* **2005**, *535*, 73−78.

(13) Liger-Belair, G.; Villaume, S.; Cilindre, C.; Jeandet, P. Kinetics of CO_2 fluxes outgassing from champagne glasses in tasting conditions: The role of temperature. *J. Agric. Food Chem.* **2009**, *57*, 1997−2003.

(14) Mulier, M.; Zeninari, V.; Joly, L.; Decarpenterie, T.; Parvitte, B.; Jeandet, P.; Liger-Belair, G. Development of a compact CO_2 sensor based on near-infrared laser technology for enological applications. *Appl. Phys. B: Lasers Opt.* **2009**, *94*, 725−732.

(15) Pozo-Bayon, M. A.; Santos, M.; Martin-Alvarez, P. J.; Reineccius, G. Influence of carbonation on aroma release from liquid systems using an artificial throat and a proton transfer reaction-mass spectrometric technique (PTR-MS). *Flavour Fragrance J.* **2009**, *24*, 226−233.

(16) Saint-Eve, A.; Déléris, I.; Aubin, E.; Semon, E.; Feron, G.; Rabillier, J.-M.; Ibarra, D.; Guichard, E.; Souchon, I. Influence of composition (CO_2 and sugar) on aroma release and perception of mint-flavored carbonated beverages. *J. Agric. Food Chem.* **2009**, *57*, 5891−5898.

(17) Cilindre, C.; Conreux, A.; Liger-Belair, G. Simultaneous monitoring of gaseous CO_2 and ethanol above champagne glasses

via micro-gas chromatography (μGC). *J. Agric. Food Chem.* **2011**, *59*, 7317−7323.
(18) Liger-Belair, G.; Cilindre, C.; Gougeon, R.; Lucio, M.; Gebefügi, I.; Jeandet, P.; Schmitt-Kopplin, P. Unraveling different chemical fingerprints between a Champagne wine and its aerosols. *Proc. Natl. Acad. Sci. U. S. A.* **2009**, *106*, 16545−16549.
(19) Liger-Belair, G.; Bourget, M.; Pron, H.; Polidori, G.; Cilindre, C. Monitoring gaseous CO_2 and ethanol above champagne glasses: Flute versus coupe, and the role of temperature. *PLoS One* **2012**, *7*, e30628.
(20) Cain, W. S.; Murphy, C. L. Interaction between chemoreceptive modalities of odour and irritation. *Nature* **1980**, *284*, 255−257.
(21) Cometto-Muniz, J. E.; Garcia-Medina, M. R.; Calvino, A. M.; Noriega, G. Interactions between CO_2 oral pungency and taste. *Perception* **1987**, *16*, 629−640.
(22) Lugli, F.; Zerbetto, F. An introduction to bubble dynamics. *Phys. Chem. Chem. Phys.* **2007**, *9*, 2447−2456.
(23) Jones, S. F.; Evans, G. M.; Galvin, K. P. Bubble nucleation from gas cavities: A review. *Adv. Colloid Interface Sci.* **1999**, *80*, 27−50.
(24) Abraham, F. F. *Homogeneous Nucleation Theory*; Academic Press: New York, 1974.
(25) Oxtoby, D. W. Homogeneous nucleation: Theory and experiment. *J. Phys.: Condens. Matter* **1992**, *4*, 7627−7650.
(26) Wilt, P. M. Nucleation rates and bubble stability in water-carbon dioxide solutions. *J. Colloid Interface Sci.* **1986**, *112*, 530−538.
(27) Debenedetti, P. G. *Metastable Liquids*; Princeton University Press: Princeton, NJ, USA, 1996.
(28) Lubetkin, S. D. Why is it much easier to nucleate gas bubbles than theory predicts? *Langmuir* **2003**, *19*, 2575−2587.
(29) Liger-Belair, G.; Vignes-Adler, M.; Voisin, C.; Robillard, B.; Jeandet, P. Kinetics of gas discharging in a glass of champagne: The role of nucleation sites. *Langmuir* **2002**, *18*, 1294−1301.
(30) Liger-Belair, G.; Marchal, R.; Jeandet, P. Close up on bubble nucleation in a glass of champagne. *Am. J. Enol. Vitic.* **2002**, *53*, 151−153.
(31) Liger-Belair, G.; Voisin, C.; Jeandet, P. Modeling non-classical heterogeneous bubble nucleation from cellulose fibers: Applications to bubbling in carbonated beverages. *J. Phys. Chem. B* **2005**, *109*, 14573−14580.
(32) Lee, W. T.; McKechnie, J. S.; Devereux, M. G. Bubble nucleation in stout beers. *Phys. Rev. E* **2011**, *83*, 051609.
(33) Lee, W. T.; Devereux, M. G. Foaming in stout beers. *Am. J. Phys* **2011**, *79*, 991−998.
(34) Liger-Belair, G.; Parmentier, M.; Jeandet, P. Modeling the kinetics of bubble nucleation in champagne and carbonated beverages. *J. Phys. Chem. B* **2006**, *110*, 21145−21151.
(35) Uzel, S.; Chappell, M. A.; Payne, S. J. Modeling the cycles of growth and detachment of bubbles in carbonated beverages. *J. Phys. Chem. B* **2006**, *110*, 7579−7586.
(36) Shafer, N. E.; Zare, R. N. Through a beer glass darkly. *Phys. Today* **1991**, *91*, 48−52.
(37) Liger-Belair, G.; Religieux, J.-B.; Fohanno, S.; Vialatte, M.-A.; Jeandet, P.; Polidori, G. Visualization of mixing flow phenomena in champagne glasses under various glass-shape and engravement conditions. *J. Agric. Food Chem.* **2007**, *55*, 882−888.
(38) Polidori, G.; Jeandet, P.; Liger-Belair, G. Bubbles and flow patterns in champagne glasses. *Am. Sci* **2009**, *97*, 294−301.
(39) Liger-Belair, G.; Bourget, M.; Villaume, S.; Jeandet, J.; Pron, H.; Polidori, G. On the losses of dissolved CO_2 during champagne serving. *J. Agric. Food Chem.* **2010**, *58*, 8768−8775.
(40) Liger-Belair, G.; Parmentier, M.; Cilindre, C. More on the losses of dissolved CO_2 during champagne serving: Toward a multiparameter modeling. *J. Agric. Food Chem.* **2012**, *60*, 11777−11786.
(41) Caputi, A.; Ueda, M.; Walter, P.; Brown, T. Titrimetric determination of carbon dioxide in wine. *Am. J. Enol. Vitic.* **1970**, *21*, 140−144.
(42) Liger-Belair, G. Nucléation, ascension et éclatement d'une bulle de champagne. *Ann. Phys. (Paris)* **2006**, *31*, 1−133.